

Real-time dual frequency comb spectroscopy in the near infrared

F. Zhu, T. Mohamed, J. Strohaber, A. A. Kolomenskii, Th. Udem, and H. A. Schuessler

Citation: [Applied Physics Letters](#) **102**, 121116 (2013); doi: 10.1063/1.4799282

View online: <http://dx.doi.org/10.1063/1.4799282>

View Table of Contents: <http://scitation.aip.org/content/aip/journal/apl/102/12?ver=pdfcov>

Published by the [AIP Publishing](#)

Articles you may be interested in

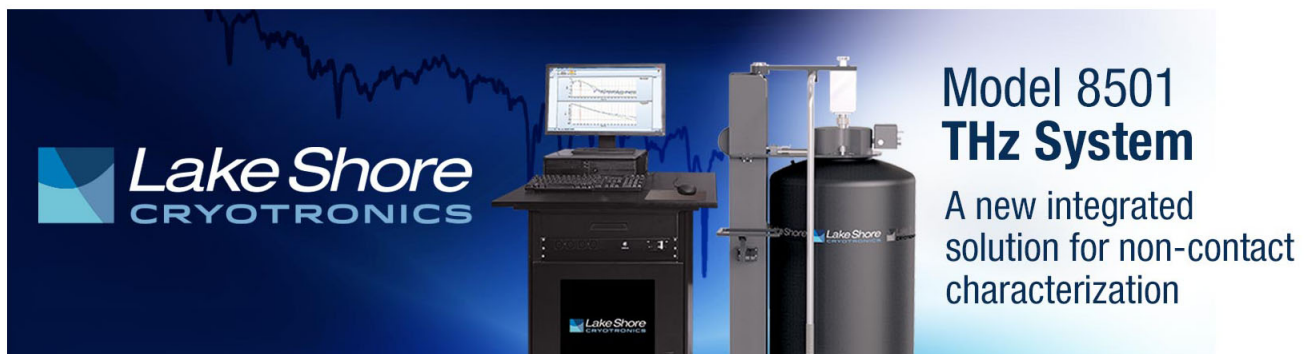
[A discretely tunable multifrequency source injection locked to a spectral-mode-filtered fiber laser comb](#)
Appl. Phys. Lett. **97**, 141107 (2010); 10.1063/1.3497080

[In situ real-time monitoring of biomolecular interactions by using surface infrared spectroscopy](#)
J. Appl. Phys. **105**, 102039 (2009); 10.1063/1.3116611

[Femtosecond real-time single-shot digitizer](#)
Appl. Phys. Lett. **91**, 161105 (2007); 10.1063/1.2799741

[Widely tunable L-band erbium-doped fiber laser with fiber Bragg gratings based on optical bistability](#)
Appl. Phys. Lett. **82**, 1335 (2003); 10.1063/1.1557321

[Nd³⁺-doped fluoroaluminate glasses for a 1.3 \$\mu\$ m amplifier](#)
J. Appl. Phys. **87**, 2098 (2000); 10.1063/1.372145

The advertisement features the Lake Shore Cryotronics logo on the left, which includes a stylized blue square icon. The central image shows a computer monitor displaying a graph, a keyboard, and a large, dark, cylindrical cryogenic system with various sensors and a vertical probe. The text on the right reads 'Model 8501 THz System' in a large, bold font, followed by 'A new integrated solution for non-contact characterization' in a smaller font.

Real-time dual frequency comb spectroscopy in the near infrared

F. Zhu,^{1,a)} T. Mohamed,^{1,2,3} J. Strohaber,¹ A. A. Kolomenskii,¹ Th. Udem,⁴
 and H. A. Schuessler^{1,2}

¹ Department of Physics and Astronomy, Texas A&M University, College Station, Texas 77843-4242, USA

² Science Department, Texas A&M University at Qatar, Doha 23874, Qatar

³ Physics Department, Faculty of Science, Beni-Suef University, Beni Suef 62511, Egypt

⁴ Max-Planck-Institut für Quantenoptik, 85748 Garching, Germany

(Received 10 January 2013; accepted 19 March 2013; published online 29 March 2013)

We use two femtosecond lasers with slightly different repetition rates to perform real-time dual frequency comb spectroscopy in the near infrared. The difference between the repetition rates is $\delta = 4403$ Hz, yielding a minimal time interval between subsequently measured interferograms and spectra of 0.227 ms. It takes as short as $4 \mu\text{s}$ to record a single interferogram, opening the possibility of studying dynamical processes. We work with different spectral outputs from two Erbium-doped fiber lasers and employ a grating based spectral filter in a $2f$ - $2f$ setup to select the common spectral region of interest, thereby increasing the signal-to-noise ratio. © 2013 American Institute of Physics. [<http://dx.doi.org/10.1063/1.4799282>]

Ever since the femtosecond frequency comb was invented in the late 1990s,¹ there have been ongoing revolutions in the field of spectroscopy. Many methods have been and are being developed to utilize the regular comb structure of millions of laser modes in spectroscopy ranging from the extreme ultraviolet to mid-infrared.^{2–6} Among these, dual frequency comb spectroscopy (DFCS) emerges as a promising, highly sensitive, and superior fast spectroscopy with high resolution to complement the traditional Fourier Transform Spectroscopy (FTS).^{2,7–16} Especially in the near and mid-infrared, a plethora of greenhouse and other gases have molecular fingerprint spectra that can be studied with DFCS based mainly on Er- or Yb-fiber lasers and their wavelength ranges extended by optical parametric oscillation processes, supercontinuum, or difference frequency generation.^{17–19}

DFCS uses two femtosecond frequency combs with slightly different repetition rates. In the time domain, pulse pairs arrive at a photo detector (PD) with a linearly increasing time delay. Each time a pulse pair overlaps in time, like for the zero path difference in FTS, the center burst of an interferogram is formed. Subsequent pulse pairs impinge on the PD with varying delay, analogous to the delay in FTS, *albeit* without moving mirror parts. As a result, the PD records an interferogram formed by many pulse pairs of various delay. Because pulse pairs repeatedly move through each other, a new interferogram starts to form after the previous is completed. In the frequency domain, comb lines of one source beat with the comb lines of the other source with slightly different line spacing, and the optical frequency information is down converted to the radio frequency range, which is the Fourier transform of the interferogram. After frequency up conversion and calibration, the optical spectrum is recovered.

Compared to traditional FTS, DFCS is extremely fast, and it was reported that an interferogram can be recorded in tens of microseconds, and time interval between subsequently

measured interferograms are several milliseconds.^{10,13} A fast oscilloscope can display an interferogram and the broadband spectrum by Fast Fourier Transform (FFT) in real time. To obtain a longer coherent interference signal (about several seconds), the repetition rates and carrier envelope offset (CEO) frequencies of both combs are stabilized. The signal record then can be transformed to a spectrum with high resolution at high signal-to-noise ratio (SNR) or be reconstructed to get the free induction decay (FID) response in the time domain.^{8,11,14} Because DFCS requires two comb sources, most of the applications employed two identical ones. In this Letter, we present results of DFCS with two spectrally different comb sources and demonstrate real-time spectroscopy with interferogram recording as short as $4 \mu\text{s}$, opening the possibility of monitoring dynamical processes. In addition, we implement a grating based spectral filtering method to increase the SNR.

Our experimental setup is depicted in Fig. 1. Fiber comb 1 (Menlo Systems, M-comb) is a femtosecond Er-doped fiber oscillator with an output power of ~ 25 mW. Fiber comb 2 (Menlo Systems, M-fiber) is a similar oscillator with an Er-doped fiber amplifier. The amplified pulse is coupled into a highly nonlinear fiber to generate a red-shifted Raman soliton. The blue part of the spectrum acquires oscillations due to self-phase modulation. The total output power is ~ 500 mW. Both fiber combs operate at repetition rates locked to frequencies of ~ 250 MHz, and their CEO frequencies are not stabilized. The auto-correlation traces and spectra of both combs are depicted in the insets of Fig. 1. The pulse durations are ~ 70 fs and ~ 90 fs for fiber combs 1 and 2, respectively. The laser beam from fiber comb 2 passes through a 20 cm long gas cell filled with a C_2H_2 and air mixture and overlaps spatially with the beam from fiber comb 1 with a polarizing beam splitter (PBS) cube.

To reduce noise in earlier work, tunable narrow-bandwidth bandpass filters were used, and the broadband spectrum was stitched together.⁸ This method provides high SNR, but requires more time; therefore, it is not ideal for real-time measurements. A prism can serve as a tunable

^{a)} Author to whom correspondence should be addressed. Electronic mail: zhuf@physic.tamu.edu

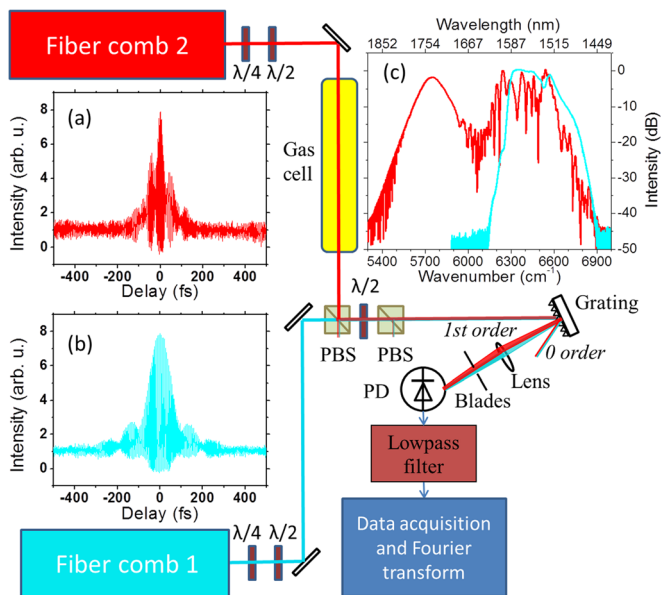


FIG. 1. Experimental setup includes two fiber lasers, waveplates and polarizers allowing to independently adjust the powers of the beams, a $2f$ - $2f$ spectral filter, and a photodetector with electronics. Interferometric autocorrelation traces are shown in inset (a) for fiber comb 2 (red) and (b) for fiber comb 1 (cyan), and inset (c) shows their respective spectra.

filter, which has a bandwidth limit.¹⁴ We employ a grating based spectral filter in a $2f$ - $2f$ configuration, which is simple, versatile, and compatible with real-time measurements. The bandwidth of the filter is easily controlled and tuned to cover the whole spectral region of interest. To achieve this, the overlapped laser beams of ~ 1 mm spot size are directed to a grating (Thorlabs, GR13-0616, 600 groove/mm, and $1.6 \mu\text{m}$ blaze). The first order diffraction is focused by a lens of focal length f (40 mm) positioned $2f$ away from the grating. To select the spectral region of interest, two blades on translational stages are placed in the focal plane of the lens as an adjustable slit. The PD is placed $2f$ away from the lens to detect the beams recombined within the selected spectral slice.²⁰ For the overlapped spectral region of ~ 80 nm between two fiber combs, corresponding to the bandwidth of fiber comb 1, the slit width is ~ 2 mm. With an optical spectrum analyzer (Yokogawa, AQ6375), we measured for our filter the roll-off of ~ 7 dB/nm and the extinction ratio of better than 0.1%.

To acquire spectral data, the difference between the repetition rates of the two fiber combs is first set at $\delta = 1807$ Hz. This value should be sufficiently low to avoid the full bandwidth of fiber comb modes beating at frequencies larger than half of the repetition rate, while it is large enough to allow for a fast recording time. To reduce aliasing, a low pass filter (DC-140 MHz) is used to filter out frequencies higher than half of the repetition rate. Interferograms are recorded for $40 \mu\text{s}$ with a Tektronix DPO 3054 oscilloscope at a sampling rate of 250 MHz with ~ 10 bits resolution. The InGaAs PD (Thorlabs, PDA10CF) has a bandwidth of 150 MHz and shows saturation behavior above 3.0 V. The specified root mean square noise is 1.4 mV. Assuming that the typical amplitude of the interferogram is about 800 mV, the PD sets the dynamic range limit of the system to ~ 570 (55 dB in signal power).

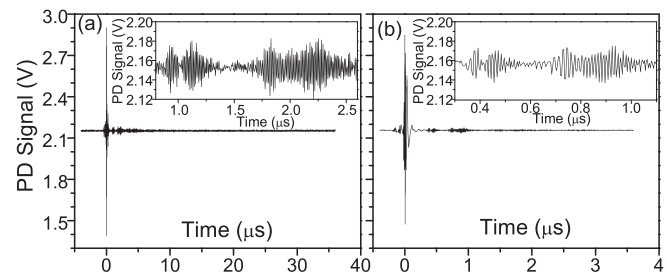


FIG. 2. Two typical interferograms: (a) $40 \mu\text{s}$ interferogram ($\delta = 1807$ Hz); (b) $4 \mu\text{s}$ interferogram ($\delta = 4403$ Hz). (Details in the text.) Insets: expanded view of the FID tail.

A typical $40 \mu\text{s}$ interferogram is shown in Fig. 2(a). The center burst of the interferogram corresponds to the temporal overlap of the pulses from the two combs. Because only the laser beam of the fiber comb 2 passes through the gas cell, the FID tail can be seen on one side of the center burst.

Figure 3 shows spectra retrieved by FFT of the corresponding single interferogram recorded for $40 \mu\text{s}$. Since in our real-time spectroscopy, the CEO frequencies are not known, recordings of the spectra are calibrated against two prominent, well-separated spectral peaks of C_2H_2 from the HITRAN database.²¹ In Fig. 3(a), the spectral measurements by DFCS are shown: (1) with spectral filtering between $6280 \sim 6625 \text{ cm}^{-1}$ (blue), corresponding to the bandwidth of fiber comb 1, and (2) between $6460 \sim 6625 \text{ cm}^{-1}$ (maroon), corresponding to the spectral fingerprint interval of acetylene ($\nu_1 + \nu_3$ band). For both measurements, the powers of the two beams reaching the PD were made equal and held constant at a level below saturation of the PD. Choosing similar spectral bandwidths and powers with filtering result in nearly

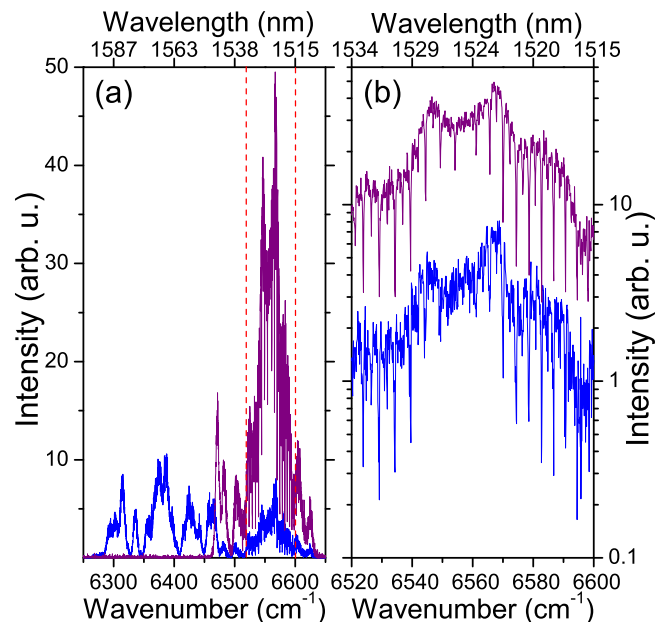


FIG. 3. Spectra retrieved from $40 \mu\text{s}$ interferograms: (a) with spectral filtering between $6280 \sim 6625 \text{ cm}^{-1}$ (blue), and between $6460 \sim 6625 \text{ cm}^{-1}$ (maroon) corresponding to the spectral fingerprint interval of acetylene are shown. A six-fold beat signal increase is achieved when using narrower spectral filtering (details in the text). (b) A magnified view of the spectral region indicated by dashed vertical lines in panel (a) presented on a logarithmic scale. The spectrum with narrower spectral filtering (maroon) shows clearer spectral features with less noise.

equal amplitudes of the spectral components of the two combs. For measurement (2), when selecting only the fingerprint spectral region, a ~ 6 times stronger spectral signal is obtained, because spectral filtering allows increasing power in the desired spectral region. Fig. 3(b) shows the central portion of the spectra on a logarithmic scale, demonstrating a measured ~ 3 fold improvement of the SNR with narrower filtering.

To extract the normalized spectrum, we first take the absorption spectrum with the C_2H_2 ($\sim 7\%$) and air ($\sim 93\%$) mixture at atmospheric pressure and room temperature. Then, we use dry air to purge the gas cell and measure the reference spectrum under the same conditions. The spectral transmittance is shown in Figs. 4(a) and 4(c). A comparison with calculations using the HITRAN database²¹ shows good agreement.

By narrowing the spectral region to the interval of interest, the difference between the repetition rates could be increased to $\delta = 4403$ Hz, which reduces the minimal time interval between subsequently measured interferograms to 0.227 ms ($1/\delta$). Experimentally, we determined that the shortest recording time which still preserves rotational lines in the fingerprints spectrum (~ 165 cm^{-1} or ~ 40 nm bandwidth) is about $4 \mu s$. A typical $4 \mu s$ interferogram is presented in Fig. 2(b). The spectral transmittance and

comparison with the HITRAN calculation is presented in Figs. 4(b) and 4(d).

We compare the normalized spectra recorded from 6460 to 6625 cm^{-1} for two cases: (1) $40 \mu s$ recording ($\delta = 1807$ Hz) with 0.11 cm^{-1} resolution, the number of spectral elements is 1500. By evaluating the root mean square noise level at positions where no signal is detected, the SNR of the most intense line is ~ 30 . (2) $4 \mu s$ recording ($\delta = 4403$ Hz) with 0.47 cm^{-1} resolution, the number of spectral elements is 351, and the SNR is ~ 80 . With these parameters, we evaluate the quality factor introduced in Ref. 12, which is the product of the number of spectral elements and the SNR normalized by the square root of the total acquisition time ($2/\delta$) counting both absorption and reference scans. For both cases, we obtain an experimental quality factor of $\sim 1.3 \times 10^6$ $Hz^{1/2}$, which follows the “spectroscopic trading rules” in Ref. 22, and is similar to the values of the previous works.^{8–10,12}

Due to the reduced comb powers in some portions of spectrum, the SNRs of these areas are less.^{5,12,14} The spectrum of Fiber comb 1 (Fig. 1(c)) has a valley in the region between 6500 \sim 6600 cm^{-1} , experimentally the SNRs at the bottom of this region in the current spectrally different setup are better than in the setup with two similar comb sources of Fiber comb 1.

Because of the pulse to pulse jitter, the intensity profile fluctuates, which results in noise of different parts of the normalized spectrum as the absorption and reference spectra are not recorded simultaneously. When precision measurements are needed, this can be improved by stabilizing the CEO frequencies of both combs, and recording/averaging interferograms over a longer time.^{8,14} In addition, an adaptive sampling scheme is being developed to achieve high-fidelity real-time DFCS.¹⁶

Although real-time DFCS needs to overcome some technical challenges (such as developing a low noise PD with large bandwidth and high dynamic range, comb sources with low intensity noise and spectrally flat, phase-coherent broad spectra) the fast and simple scheme is promising for the rapid identification of many molecular species simultaneously and in real time. By further increasing the repetition rates of dual combs, or decreasing the bandwidth of spectral of interest with a $2f-2f$ filter, the repetition rate difference (δ) can be further increased, which will further reduce the minimal time interval between subsequently measured interferograms ($1/\delta$). The short measuring time and time interval open the possibility to study combustion phenomena,²³ and other dynamical processes. The sensitivity can be further improved with such techniques as cavity¹⁰ or multipass signal enhancement¹⁴ to characterize minute trace amounts of molecules.

We thank Menlo Systems for the generous loan of the M-comb. This work was funded by the Robert A. Welch Foundation Grant No. A1546, and the NSF Grant No. 1058510.

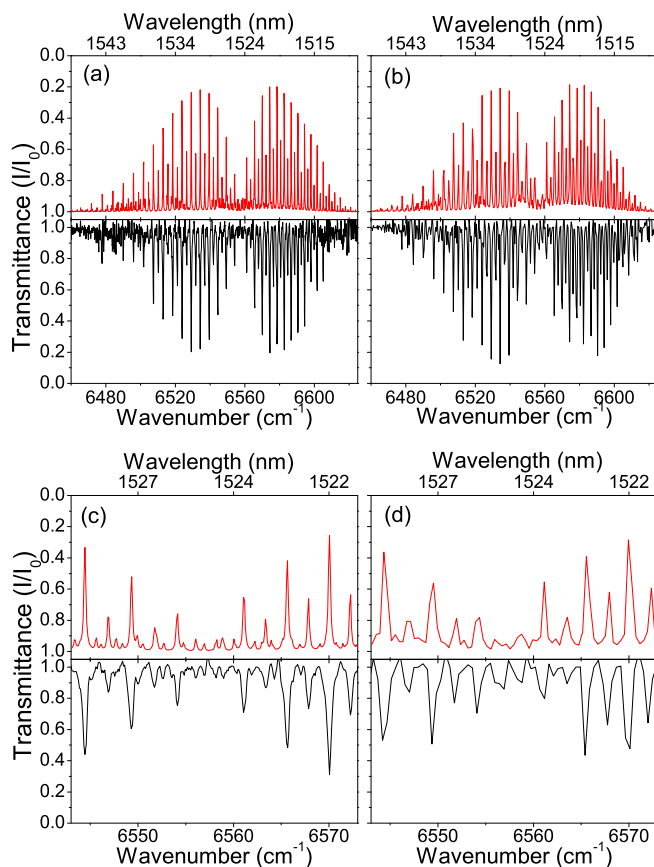


FIG. 4. Normalized DFCS spectra of acetylene (black) compared to spectra calculated with the HITRAN data base of different resolution accordingly (red, inverted for clarity): in the broad range between 6460 \sim 6625 cm^{-1} , (a) $40 \mu s$ interferogram ($\delta = 1807$ Hz); (b) $4 \mu s$ interferogram ($\delta = 4403$ Hz); expanded view between 6543 \sim 6573 cm^{-1} , (c) $40 \mu s$ interferogram ($\delta = 1807$ Hz); and (d) $4 \mu s$ interferogram ($\delta = 4403$ Hz).

¹Th. Udem, R. Holzwarth, and T. W. Hänsch, *Nature* **416**, 233 (2002).

²F. Keilmann, C. Gohle, and R. Holzwarth, *Opt. Lett.* **29**, 1542 (2004).

³S. A. Diddams, L. Hollberg, and V. Mbele, *Nature* **445**, 627 (2007).

⁴C. Gohle, B. Stein, A. Schliesser, Th. Udem, and T. W. Hänsch, *Phys. Rev. Lett.* **99**, 263902 (2007).

- ⁵A. Foltynowicz, T. Ban, P. Maslowski, F. Adler, and J. Ye, *Phys. Rev. Lett.* **107**, 233002 (2011).
- ⁶A. Cignöz, D. C. Yost, T. K. Allison, A. Ruehl, M. E. Fermann, I. Hartl, and J. Ye, *Nature* **482**, 68 (2012).
- ⁷A. Schliesser, M. Brehm, and F. Keilmann, *Opt. Express* **13**, 9029 (2005).
- ⁸I. Coddington, W. C. Swann, and N. R. Newbury, *Phys. Rev. Lett.* **100**, 013902 (2008).
- ⁹P. Giaccari, J. D. Deschenes, P. Saucier, J. Genest, and P. Tremblay, *Opt. Express* **16**, 4347 (2008).
- ¹⁰B. Bernhardt, A. Ozawa, P. Jacquet, M. Jacqey, Y. Kobayashi, Th. Udem, R. Holzwarth, G. Guelachvili, T. W. Hänsch, and N. Picqué, *Nat. Photonics* **4**, 55 (2010).
- ¹¹I. Coddington, W. C. Swann, and N. R. Newbury, *Opt. Lett.* **35**, 1395 (2010).
- ¹²N. R. Newbury, I. Coddington, and W. C. Swann, *Opt. Express* **18**, 7929 (2010).
- ¹³B. Bernhardt, E. Sorokin, P. Jacquet, R. Thon, T. Becker, I. T. Sorokina, N. Picqué, and T. W. Hänsch, *Appl. Phys. B* **100**, 3 (2010).
- ¹⁴A. M. Zolot, F. R. Giorgetta, E. Baumann, J. W. Nicholson, W. C. Swann, I. Coddington, and N. R. Newbury, *Opt. Lett.* **37**, 638 (2012).
- ¹⁵J. Roy, J. Deschenes, S. Potvin, and J. Genest, *Opt. Express* **20**, 21932 (2012).
- ¹⁶T. Ideguchi, A. Poisson, G. Guelachvili, T. W. Hänsch, and N. Picqué, *Opt. Lett.* **37**, 4847 (2012).
- ¹⁷Z. Zhang, C. Gu, J. Sun, C. Wang, T. Gardiner, and D. T. Reid, *Opt. Lett.* **37**, 187 (2012).
- ¹⁸T. W. Neely, T. A. Johnson, and S. A. Diddams, *Opt. Lett.* **36**, 4020 (2011).
- ¹⁹A. Schliesser, N. Picqué, and T. W. Hänsch, *Nat. Photonics* **6**, 440 (2012).
- ²⁰I. G. Mariyenko, J. Strohaber, and C. J. G. J. Uiterwaal, *Opt. Express* **13**, 7599 (2005).
- ²¹L. S. Rothman, I. E. Gordon, A. Barbe, D. Chris Benner, P. F. Bernath, M. Birk, V. Boudon, L. R. Brown, A. Campargue, J. P. Champion, K. Chance, L. H. Coudert, V. Dana, V. M. Devi, S. Fally, J. M. Flaud, R. R. Gamache, A. Goldman, D. Jacquemart, I. Kleiner, N. Lacome, W. J. Lafferty, J. Y. Mandin, S. T. Massie, S. N. Mikhailenko, C. E. Miller, N. Moazzen-Ahmadi, O. V. Naumenko, A. V. Nikitin, J. Orphal, V. I. Perevalov, A. Perrin, A. Predoi-Cross, C. P. Rinsland, M. Rotger, M. Simeckova, M. A. H. Smith, K. Sung, S. A. Tashkun, J. Tennyson, R. A. Toth, A. C. Vandaele, and J. Vander Auwera, *J. Quantum Spectrosc. Radiat. Transfer* **110**, 533 (2009).
- ²²P. R. Griffiths and J. A. de Haseth, *Fourier Transform Infrared Spectrometry* (Wiley, 2007).
- ²³M. Valorani, H. N. Najm, and D. A. Goussis, *Combust. Flame* **134**, 35 (2003).